

Physical gels of telechelic triblock copolymers with precisely defined junction multiplicity†

Paulina J. Skrzyszewska,^{*ab} Frits A. de Wolf,^c Marc W. T. Werten,^c Antoine P. H. A. Moers,^c Martien A. Cohen Stuart^a and Jasper van der Gucht^a

Received 7th November 2008, Accepted 27th February 2009

First published as an Advance Article on the web 31st March 2009

DOI: 10.1039/b819967a

We study transient networks formed by monodisperse telechelic polypeptides with collagen-like end blocks and a random-coil-like middle block. These artificial proteins are created using recombinant DNA techniques. Upon cooling, the end blocks associate reversibly into triple helices, leading to gels with a well-defined junction multiplicity of three. Both the storage modulus and the relaxation time of the gel increase very strongly as a function of concentration, and decrease with increasing temperature. All the experimental results are described quantitatively by an analytical model, based on classical gel theory, that requires no adjustable parameters, and accounts for the molecular structure of the gel, and the presence of loops and dangling ends.

1. Introduction

Polymer gels, due to their properties, have many applications, for example as drug delivery systems,¹ wound dressing materials,² and rheological regulators in polymer blends.³ In general, two classes of gels can be distinguished. Permanent gels are formed by strong covalent cross-links. They do not restructure or flow. By contrast, physical or reversible gels are formed by weak interactions such as hydrogen bonds, van der Waals forces, hydrophobic or electrostatic interactions. These gels have the possibility to restructure. Moreover the cross-links can respond to changes in conditions, such as temperature, concentration, or pH. Examples of thermoreversible physical gels are gelatin and agarose⁴ (formed upon cooling) or polymethacrylic acid⁴ and methyl cellulose⁵ (formed upon heating).

An interesting class of physical gels is formed by associative telechelic polymers. These are triblock copolymers with groups at their ends that can reversibly assemble into supramolecular knots. The middle block has hydrophilic character and serves as a spacer. A lot of research has been devoted to water-soluble polymers (such as PEO) terminated with hydrophobic groups at both ends.^{6,7} These molecules form reversible networks in which the junction points consist of micelles formed by association of the hydrophobic end groups. Other examples of associating telechelic polymers are biosynthetic protein polymers with end groups inspired by the natural protein elastin, which associate by hydrophobic interactions,^{8,9} and protein polymers with leucine

zipper domains at the ends, which aggregate by coiled-coil interactions.^{10,11}

Associative telechelic polymers serve as model molecules for studying the structure and rheological behavior of physical gels. Qualitatively, the network formation in these systems and their dynamics can be understood from theoretical models that take into account intra- and intermolecular associations, as well as the transient character of the cross-links.^{12,13} However, quantitative modeling is very difficult for the systems that have been studied so far, because the multiplicity of the nodes is not controlled and invariably polydisperse.

In this paper we study a new class of thermoreversible gels,¹⁴ in which the node multiplicity is precisely known. The gel network is formed by a telechelic polypeptide¹⁴ with (Pro-Gly-Pro)₉ end blocks inspired by, and behaving like, natural collagen,¹⁵ while the middle block (399 amino acids long) is rich in hydrophilic amino acids and assumes a random-coil structure in water over

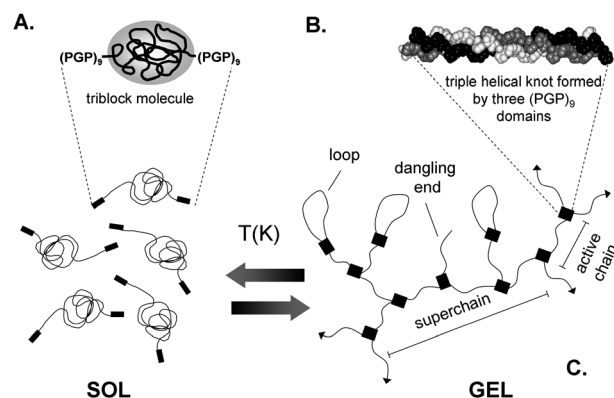


Fig. 1 Gel network formation by telechelic polypeptides: (A) single polypeptide consisting of a random-coil-like middle block flanked by collagen-like end blocks (G—glycine, P—proline); (B) triple helical knot formed by three end blocks; (C) gel network formed reversibly upon cooling. Chains terminated with an arrow are connected to the percolated gel network.

^aLaboratory of Physical Chemistry and Colloid Science, Wageningen University, Dreijenplein 6, 6703 HB Wageningen, The Netherlands. E-mail: paulina.skrzyszweska@wur.nl; Fax: (+31) (0)317 483 777; Tel: +31 (0)317-485595

^bDutch Polymer Institute (DPI), P.O. Box 902, 5600 AX Eindhoven, The Netherlands

^cBiobased Products, Agrotechnology & Food Sciences Group, Bornsesteeg 59, 6708 PD Wageningen, The Netherlands

† Electronic supplementary information (ESI) available: Differential scanning calorimetry results. See DOI: 10.1039/b819967a

a wide range of temperatures (Fig. 1A). The polypeptide is produced by genetically modified yeast (*Pichia pastoris*), and is monodisperse, having a defined length and amino acid sequence. Below the melting temperature, the side blocks assemble and form triple helices in a reversible manner (see Fig. 1B), while the middle block maintains a random-coil structure. Stable junction points can only be formed when three collagen-like side blocks form a triple helix, as double helices are not stable. As a consequence, a physical gel is formed in which the node multiplicity is exactly three (see Fig. 1C). As we will show this well-defined multiplicity allows us to model the network properties quantitatively.

In addition to being an ideal model system for studying the relation between structure and rheology of physical gels, the investigated system could also provide an improved alternative for gelatin in, for example, medical, pharmaceutical, food, or cosmetic applications. Conventional gelatin, derived from partially hydrolyzed and chemically modified animal collagen, is susceptible to a risk of contamination with prions or viruses and a risk of eliciting allergic reactions, particularly against the non helix-forming domains of collagen. The molecules studied here, produced in microbial cells, eliminate those risks.

In this paper we investigate the viscoelastic properties of these collagen-inspired telechelic polypeptides as a function of polymer concentration and temperature. To explain the experimental data, an analytical model is developed, that takes into account the multiplicity of the network and the transient character of the triple helical junctions.

2. Materials and methods

The recombinant protein (TR₄T) was prepared by inserting an artificial gene into the genome of *P. pastoris* and then produced in a fed-batch fermentation process.¹⁴ Purification consists of several precipitation steps and desalting. More details can be found in ref. 14. The protein has a molecular weight of ~42 kDa and comprises three blocks (Fig. 1A). The end blocks, abbreviated as T (trimer-forming), consist of nine consecutive Pro-Gly-Pro triplets.¹⁴ Such (Pro-Gly-Pro)_n stretches are known to form collagen-like triple helices.¹⁶ The middle block R₄ (399 amino acids) has a sequence that does not lead to any secondary or tertiary structure; it assumes a random-coil configuration.¹⁴ The amino acid sequence of the middle block corresponds to a randomized version of the sequence of the previously described P₄ block,¹⁷ in such a way that glycine is *not* every third residue, thus preventing triple helix formation. Accordingly, it was previously shown by circular dichroism spectroscopy and differential scanning calorimetry that exclusively the end blocks participate (near-quantitatively) in triple helix formation.¹⁴ The amino acid sequences of the TR₄T triblock protein and of a separately produced protein corresponding to the R₄ middle block have been deposited in GenBank under accession numbers ACF33479 and ACF33477, respectively.

Four different concentrations of protein were tested (0.96, 1.1, 1.3 and 1.4 mM). All samples were prepared in the same way. A given amount of protein was dissolved in phosphate buffer (pH 7, I = 10 mM) and then heated at 50 °C for half an hour, allowing the protein to dissolve completely under conditions where no triple helices form.

The rheological measurements were made using an Anton Paar, Physica MCR 301 rheometer equipped with a cone and plate geometry of 50 mm diameter. The temperature was controlled by a Peltier system, which allowed fast heating and cooling. A solvent trap was used to minimize evaporation. Before adding the warm protein solution, the plate was preheated to 50 °C. After lowering the cone, the system was quenched to 20 °C. Gel formation was monitored by applying a sinusoidal deformation to the system ($f = 1$ Hz and $\gamma = 1\%$) and determining the storage (G') and loss (G'') moduli. It was checked that this deformation does not influence the kinetics of gel formation. Viscoelastic dynamic characterization of the steady state gel was performed in a frequency range 0.001–20 Hz (0.00628–125 rad/s) and with a deformation amplitude of 1%, well within the linear response regime. Creep experiments were carried out at different applied stresses between 5 and 20 Pa, depending on protein concentration. The stress values were chosen not to go beyond the linear regime. The duration of the deformation phase was 1800 s, which was followed by 1800 s of recovery. Creep experiments were done at different temperatures. After the gel was formed at 20 °C, the temperature was decreased in steps to 15, 10 and 5 °C. At each temperature, the system was equilibrated for 4 hours, before doing measurements.

3. Experimental results

At temperatures above 50 °C, solutions of TR₄T were viscous without detectable elastic response. When the sol was cooled down to 20 °C a physical gel was formed as a result of triple helix formation by the collagen-like end blocks. Fig. 2 displays the development of the storage (G') and loss (G'') moduli for a 1.4 mM solution. In the beginning, viscous properties are dominant and the system does not show any gel-like behavior. With time, as the gel forms, the elastic properties start to play a more important role. After some time (~12 min) G' and G'' cross. The steady state is reached after approximately 6 hours. The same type of experiment with the R₄ block only (hence without helix-forming ends) showed no development of the storage modulus with time (Fig. 2). From this, we conclude that the network formation is a consequence of triple helix formation by the end blocks, and not caused by entanglements.

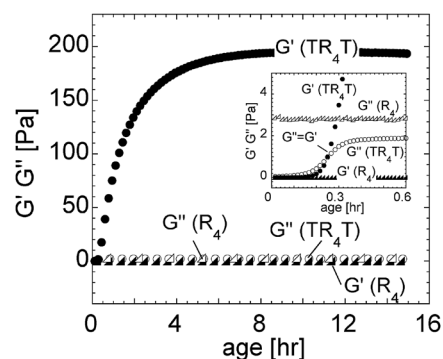


Fig. 2 Storage (●) and loss (○) moduli for 1.4 mM TR₄T; storage (▲) and loss (△) moduli for 1.4 mM R₄ as a function of age (1 Hz, $\gamma = 1\%$). Inset presents a zoomed view of the initial stage of gelation.

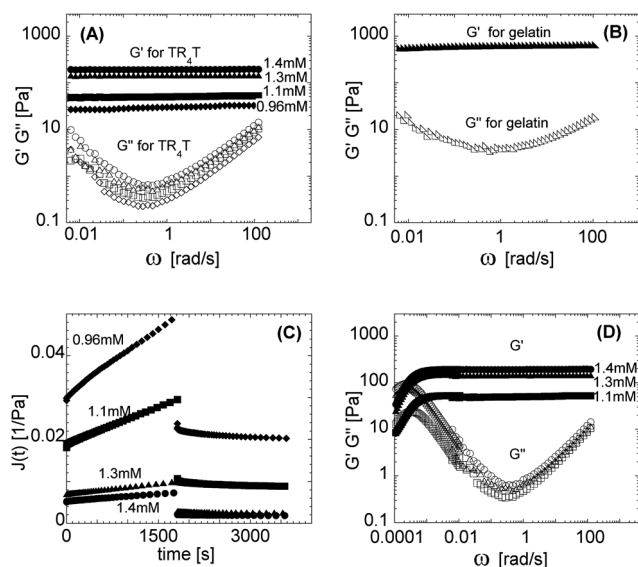


Fig. 3 (A) Frequency sweeps at $T = 293$ K for different concentrations as indicated; (B) frequency sweep for 50 g/l of gelatin at $T = 293$ K; (C) creep experiments at 293 K for different concentrations as indicated; (D) combined frequency sweeps and converted creep experiments from parts A and C.

The dynamic, viscoelastic behavior of the stable gel was investigated by means of frequency sweeps. Storage and loss moduli as a function of frequency for different protein concentrations are presented in Fig. 3A. In all cases the elastic behavior (G') dominates over the viscous behavior (G''). The storage modulus does not depend on frequency in the range between 0.01 and 100 rad/s. The loss modulus initially decreases with frequency, goes through a minimum and then increases again. We note that gelatin has a similar viscoelastic response (Fig. 3B).

In order to gain insight into the system on time scales above 100 s, creep experiments were done. A constant stress was applied to the gel and the resulting deformation was measured as a function of time. Deformation is expressed as a time dependent compliance $J(t)$ (strain divided by applied stress). Creep curves (Fig. 3C) are characterized by a rapid elastic response followed by a slow viscous response. When the stress is removed, the elastic response is recovered. The creep curves are rather accurately, although not exactly, described by a single-relaxation time Maxwell model, $J(t) = 1/G_0 + t/\eta$, where G_0 is the elastic modulus and η is the zero-shear viscosity. This was expected, since many transient networks obey Maxwell behavior.⁶ The creep data were converted to the frequency domain by a method described by Ferry.¹⁸ Together with the frequency sweeps presented in Fig. 3A, this gives the viscoelastic behavior of the system over a broad frequency range, comprising six decades (Fig. 3D).

From the data presented in Fig. 3, we obtain the plateau modulus G_0 , the zero-shear viscosity η (the inverse slope of $J(t)$ at long deformation times), and the relaxation time of the gels τ (η divided by G_0). These parameters are plotted as a function of concentration and temperature in Fig. 4 and 5. In these figures, the symbols represent the experimental data, while the solid lines correspond to model calculations, described in section 4.

Fig. 4A shows the plateau modulus (G_0) as a function of concentration at different temperatures. Clearly, the storage

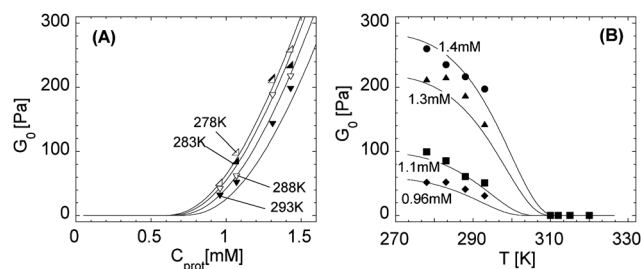


Fig. 4 (A) Storage modulus as a function of concentration of protein (C_{prot}) at different temperatures: (\blacktriangledown) 293 K, (\triangledown) 288 K, (\blacktriangle) 283 K, (\triangle) 278 K; (B) storage modulus as a function of temperature for different concentrations (C_{prot}): (\bullet) 1.4 mM, (\blacktriangle) 1.3 mM, (\blacksquare) 1.1 mM, (\blacklozenge) 0.96 mM. In both figures, solid lines correspond to model calculations described in section 4.

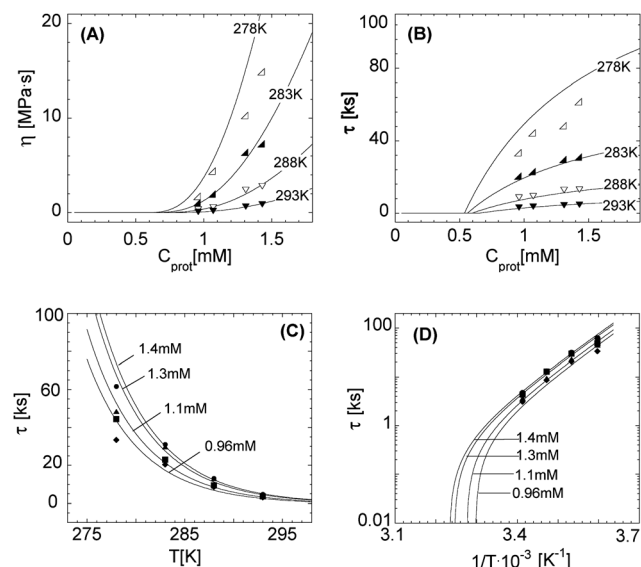


Fig. 5 (A) η as a function of concentration at different temperatures: (\blacktriangledown) 293 K, (\triangledown) 288 K, (\blacktriangle) 283 K, (\triangle) 278 K; (B) τ as a function of concentration at the same temperatures; (C) τ as a function of temperature for different concentrations: (\bullet) 1.4 mM, (\blacktriangle) 1.3 mM, (\blacksquare) 1.1 mM, (\blacklozenge) 0.96 mM; (D) Arrhenius plot of τ for the same concentrations. In all figures, the solid lines correspond to model calculations described in section 4.

modulus depends strongly on concentration. Below $C_{\text{prot}} \approx 0.9$ mM the gel is very weak, probably being close to a percolation threshold. At a concentration of 1.4 mM it already has a significant storage modulus of ~ 250 Pa. The temperature dependency is presented in Fig. 4B. At $T > 310$ K there is no measurable storage modulus, while at low temperatures the modulus stabilizes at a plateau. Unfortunately, no reliable data between 293 and 310 K could be measured, due to problems with evaporation at the long equilibration times that were needed. In fast, non-equilibrium heating experiments (~ 1.6 K/min), the modulus decreased to zero at temperatures between 300 and 310 K, but the real (equilibrium) melting temperature is probably somewhat lower. Note that the temperature at which the gel properties disappear is lower than the melting temperature of the triple helices as measured with calorimetry (around 315 K, see supporting information and ref. 14).

As can be seen in Fig. 5, both η and τ increase with decreasing temperature and increasing protein concentration (C_{prot}).

Fig. 5D is an Arrhenius plot of the relaxation time, showing that dissociation of triple helices is an activated process, characterized by an activation barrier.

The dependence of the storage modulus on the protein concentration is much stronger than for commonly known physical gels such as gelatin¹⁹ or pectins.²⁰ According to classical gel theory, the modulus is proportional to the concentration of elastically active chains, *i.e.* chains that bridge two cross-links in the gel. Our results therefore indicate that the fraction of chains that are active increases strongly with increasing concentration.

Moreover, the concentration dependence of the relaxation time (Fig. 5B) indicates that the relaxation time is not simply determined by the dissociation of a single triple helix. There must be other factors contributing to stress relaxation. Experiments above the melting temperature and experiments with the R₄ block without helix-forming blocks showed that entanglements do not contribute to the elasticity of the gels. Rather, we believe that the detailed structure of the network is responsible for the strong concentration dependence. To test this, we developed a model based on the classical network theory of Flory²¹ and Stockmayer,²² which accounts explicitly for the well-defined functionality of the network.

4. Model

Each triple helix is formed by association of three end blocks. The equilibrium constant for this process is written as:

$$K_H = \frac{C_H}{C_F^3} \quad (1)$$

where C_H is the concentration of triple helices and C_F the concentration of free end blocks. [Note that the detailed structure of the triple helix (all-ends parallel or two parallel and one antiparallel) is not important for the mechanical properties of the gel because the middle block is relatively long.] There are two possibilities to form a triple helix. It can be formed either by three end blocks from three different chains, or by three end blocks from two different chains, such that two side blocks come from the same polypeptide. The first case leads to the junction points of the network, while the second case corresponds to loops. Loops, in addition to free (dangling) ends, act as gel stoppers (see Fig. 1C). Obviously, $C_H = C_J + C_L$ with C_J the concentration of junctions and C_L that of loops.

The probability of forming a junction point (with volume ν) is $(C_F \cdot \nu)^3$, because three free end groups have to meet in a volume ν . The probability of forming a loop is $[(C_F \cdot \nu)^2] \cdot [\nu/V_{\text{coil}}] \cdot [C_F/2C_T]$. Here, the first factor is the probability that two free end groups of different chains meet, the second factor is the probability that the other end of one of these chains is also situated in the volume ν (with V_{coil} the volume of a polymer coil), and the third factor is the probability that this end is not (yet) involved in a helix, with C_T the total concentration of chains. It follows that:

$$C_L = \frac{C_J}{2 \cdot C_T \cdot V_{\text{coil}}} \approx \frac{C_J \cdot C^*}{2 \cdot C_T} \quad (2)$$

where $C^* \approx 1/V_{\text{coil}}$ is the overlap concentration. Loops are predominant below the overlap concentration C^* , while junctions are predominant for $C_T > C^*$.

For given K_H and C_T , the concentrations of free end groups (dangling ends), loops, and junctions can be calculated using eqn 1 and 2. The probability for a certain end group to be involved in a junction point is equal to $p = 3C_J/2C_T$. According to classical gel theory, the critical gelation (or percolation) threshold for a trifunctional network is at $p = 1/2$. For $p > 1/2$, a certain fraction of chains is connected to an infinite cluster. Dangling ends or loops are termination points for the cluster. The probability β that a given branch, emanating from a junction point is not connected to the infinite cluster can be calculated from the probability p . In a mean-field approximation²³ $\beta = (1 - p)/p$. The probability that all three emanating chains are connected to the infinite cluster is $(1 - \beta)^3$, while the probability that only two out of three chains are linked to the gel is $3\beta(1 - \beta)^2$.

Only junction points with all three branches linked to the gel network connect elastically active chains. Junction points with only two of their chains linked to the gel merely elongate the active chains and are responsible for the formation of so-called "superchains", active chains consisting of more than one molecule (Fig. 1C).²³

The total number of elastically active chains can be calculated as $\nu_{\text{eff}} = 1.5 \cdot C_J(1 - \beta)^3$ where the factor 1.5 takes into account that each junction has three active chains and that each active chain connects two junction points. This gives for the elastic modulus:

$$G_0 \approx F \cdot \nu_{\text{eff}} \cdot R \cdot T = F \cdot 1.5 \cdot C_J \cdot (1 - \beta)^3 \cdot R \cdot T = \frac{F \cdot [C_T \cdot (2p - 1)^3 \cdot R \cdot T]}{p^2} \quad (3)$$

Here RT is the thermal energy per mole, and F is a prefactor, the so-called front factor. In the classical, affine network theory, $F = 1$,²¹ while for the phantom network model $F = 1/3$ in the case of trifunctional nodes.²⁴ For $p = 1/2$ (percolation threshold), the modulus vanishes, while for $p = 1$ (all junctions active) we recover the classical rubber-like scaling $G_0 = F \cdot C_T \cdot R \cdot T$.

The total number of chains involved in links, *i.e.* junction points connected with at least two strands to the gel, is:

$$n = C_J \cdot [1.5 \cdot (1 - \beta)^3 + 3 \cdot \beta \cdot (1 - \beta)^2] \quad (4)$$

From this we obtain for the average length of an active chain:

$$\langle N \rangle = \frac{n}{\nu_{\text{eff}}} = \frac{1}{2p - 1} \quad (5)$$

Just above the network threshold ($p = 1/2$), that is, slightly below the melting temperature or at low concentrations, the effective active chains are much longer than a single polymer chain (we call these superchains, see Fig. 1C); for p close to unity, $\langle N \rangle$ goes to unity.

Stress relaxation occurs when an elastically active chain breaks. Here, this happens when a triple helix (junction point) dissociates. A superchain consisting of N molecules can break in N places, so its relaxation time is expected to be N times shorter than the life time τ_0 of a single helix:

$$\tau = \frac{\tau_0}{\langle N \rangle} = \tau_0 \cdot (2p - 1) \quad (6)$$

We note that τ_0 is related to the thermal dissociation rate of a triple helix $\tau_0 = k_d^{-1}$ with k_d the dissociation rate constant. For k_d we assume Arrhenius behavior:

$$k_d = k_{d,0} \cdot \exp \left[\frac{-E_a}{RT} \right] \quad (7)$$

where E_a is the activation energy. Dissociation becomes faster as the temperature increases. The equilibrium constant of helix formation is also a function of the temperature. This temperature dependence can be expressed by Van't Hoff's equation:

$$K_H = K_{H,0} \cdot \exp \left[\frac{-\Delta H}{RT} \right] \quad (8)$$

where ΔH is the molar enthalpy of helix formation. Since helix formation is an exothermic process ($\Delta H < 0$), K_H decreases with increasing temperature. The shift in equilibrium constant brings changes in C_F , C_J , and C_L and thus changes in the storage modulus, the relaxation time, and the viscosity.

The model described in this section describes the linear viscoelasticity of the network with six parameters: F , C^* , E_a , $k_{d,0}$, ΔH , and $K_{H,0}$. The front factor F was chosen as 0.5 as a trade off between the classical affine network theory and the phantom network model. The overlap concentration C^* can be calculated from the dimension of the chains. The radius of gyration R_g is estimated to be ~ 7 nm, based on a master curve for R_g as a function of the number of residues proposed by Fritzke and Rose.²⁵ Knowing that $V_{\text{coil}} = 4/3\pi R_g^3$, and that the mass of a single chain is M_{prot}/N_A , where $M_{\text{prot}} \sim 42$ kDa and N_A is Avogadro's number, we calculated the overlap concentration as $C^* = 0.0011$ M. To obtain a value for the molar enthalpy of helix formation, we performed differential scanning calorimetry measurements (see ESI†). The measured enthalpy is approximately -250 kJ/mole. This value corresponds very well with results obtained by Frank *et al.*,¹⁶ who found an enthalpy of -8.9 kJ per mole of tripeptide, corresponding to 220–250 kJ per mole of end blocks in triple helices formed. From the calorimetry data, we also obtain the prefactor $K_{H,0}$: $5 \cdot 10^{-37}$ l²/mole² (see ESI†). The activation energy E_a and the prefactor $k_{d,0}$ that specify the dissociation rate, finally, are obtained from the data in Fig. 5D. Assuming Arrhenius behavior for τ_0 (eqn 7), we find $E_a = 112 \pm 4$ kJ/mole and $k_{d,0} \approx 10^{16}$ s.

With no further adjustable parameters, we can compute G_0 , τ , and $\eta (=G_0 \cdot \tau)$ as a function of concentration and temperature. The results of these calculations are shown in Fig. 4 and 5 (drawn curves). All these curves (both concentration and temperature dependencies) are in very good agreement with the experimental data.

From the model, we deduce the internal structure of the gel in terms of the fractions of chain ends in triple helices (junctions or loops) and free ends. In Fig. 6 we present how each fraction depends on temperature and concentration. With increasing temperature, the fraction of helices decreases and that of free ends increases. Half of the helices have melted at a temperature of 315 K for a 1.4 mM solution and at 313 K for 0.96 mM. These melting temperatures were confirmed with differential scanning calorimetry (ESI†) and with measurements of the helical content using circular dichroism.¹⁴ By contrast, the elastic properties of the networks are lost at much lower temperatures, around 300 K

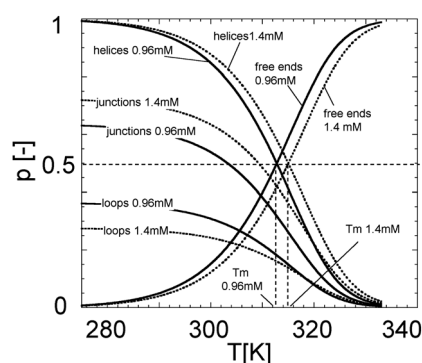


Fig. 6 Dependency of the fractions of triple helices, loops and dangling ends (as indicated) on protein concentration and temperature. Dotted curves: 1.4 mM, full curves: 0.96 mM.

(see Fig. 4B). The reason for this is that only helices involved in junctions contribute to the elastic properties; helices in loops do not. As can be seen in Fig. 6, the fraction of chain ends in junctions reaches the critical value of 1/2 at significantly lower temperatures than the total helix fraction. This effect is stronger for low polymer concentrations, because the fraction of loops increases with decreasing concentration. The latter also explains the strong concentration dependence of the modulus (Fig. 4A).

5. Concluding remarks

In this paper, we investigated a new type of telechelic polymers that self-assemble reversibly into transient networks with a node multiplicity of exactly three. The well-defined multiplicity made it possible to develop a theoretical model based on classical gel theory, which allows calculation of the complete (linear) viscoelastic behavior of the network from a limited set of input parameters, that can all be measured independently. The model calculations were in *quantitative* agreement with experiments, showing that the structure of our physical gels are rather well described by classical theory, at least not too close to the percolation threshold.

As far as we know, this is the first report which describes the internal structure of a network formed by telechelic polymer with such well-defined multiplicity. Telechelics with a multiplicity of 2 have been reported in literature, based on hydrogen-bonding,²⁶ complementary strands of DNA,²⁷ or coordination bonds,²⁸ but these molecules form only linear chains and no networks. Conventional telechelics, such as PEO chains with hydrophobic side blocks, have higher node multiplicity and do form networks. However, the number of chains emanating from a node in these systems can fluctuate around an average value. This eliminates the special features associated with a precise node multiplicity, and makes quantitative modeling more difficult.

In this paper, we considered only one polypeptide sequence, but the precise molecular design can be varied easily by changing the design of the underlying DNA template. By varying the length of the different blocks, for example, we can modify the rheological and structural properties of the networks. The collagen-inspired telechelic polypeptides studied here thus form a class of physical gels with highly controllable and predictable properties.

Acknowledgements

We would like to thank Joris Sprakel for help with the rheological measurements. We thank the Dutch Polymer Institute for financial support. This research forms part of the research program of the Dutch Polymer Institute (DPI) project #602.

References

- 1 M. Sutter, J. Siepmann, W. E. Hennink and W. Jiskoot, *Journal of Controlled Release*, 2007, **119**, 301–312.
- 2 B. Balakrishnan, M. Mohanty, P. R. Umashankar and A. Jayakrishnan, *Biomaterials*, 2005, **26**, 6335–6342.
- 3 J. Kim, S. S. Kim, K. H. Kim, Y. H. Jin, S. M. Hong, S. S. Hwang, B. G. Cho, D. Y. Shin and S. S. Im, *Polymer*, 2004, **45**, 3527–3533.
- 4 K. T. Nijenhuis, *Polymer Bulletin*, 2007, **58**, 27–42.
- 5 S. C. Lee, Y. W. Cho and K. Park, *Journal of Bioactive and Compatible Polymers*, 2005, **20**, 5–13.
- 6 T. Annable, R. Buscall, R. Ettelaie and D. Whittlestone, *Journal of Rheology*, 1993, **37**, 695–726.
- 7 J. S. Sprakel, E. Cohen Stuart, M. A. Besseling, N. A. M. Lettinga and M. P. van der Gucht, *Soft Matter*, 2008, **4**, 1696–1705.
- 8 E. R. Wright and V. P. Conticello, *Advanced Drug Delivery Reviews*, 2002, **54**, 1057–1073.
- 9 K. Nagapudi, W. T. Brinkman, B. S. Thomas, J. O. Park, M. Srinivasarao, E. Wright, V. P. Conticello and E. L. Chaikof, *Biomaterials*, 2005, **26**, 4695–4706.
- 10 W. A. Petka, J. L. Harden, K. P. McGrath, D. Wirtz and D. A. Tirrell, *Science*, 1998, **281**, 389–392.
- 11 S. B. Kennedy, K. Littrell, P. Thiyagarajan, D. A. Tirrell and T. P. Russell, *Macromolecules*, 2005, **38**, 7470–7475.
- 12 F. Tanaka and S. F. Edwards, *Macromolecules*, 1992, **25**, 1516–1523.
- 13 F. Tanaka, *Polymer Journal*, 2002, **34**, 479–509.
- 14 M. W. T. Werten, H. Teles, A. P. H. A. Moers, E. J. H. Wolbert, J. Sprakel, G. Eggink and F. A. de Wolf, *Biomacromolecules*, 2009, DOI: 10.1021/bm801299u.
- 15 G. N. Ramachandram, *Biochemistry of Collagen*, Plenum Press, New York, 1976.
- 16 S. Frank, R. A. Kammerer, D. Mechling, T. Schulthess, R. Landwehr, J. Bann, Y. Guo, A. Lustig, H. P. Bachinger and J. Engel, *Journal of Molecular Biology*, 2001, **308**, 1081–1089.
- 17 M. W. T. Werten, W. H. Wisselink, T. J. J. Jansen-van den Bosch, E. C. de Bruin and F. A. de Wolf, *Protein Engineering*, 2001, **14**, 447–454.
- 18 J. D. Ferry, *Viscoelastic Properties of Polymers*, Wiley, New York, 1980.
- 19 K. T. Nijenhuis, *Colloid and Polymer Science*, 1981, **259**, 1017–1026.
- 20 E. E. Braudo, I. G. Plashchina and V. B. Tolstoguzov, *Carbohydrate Polymers*, 1984, **4**, 23–48.
- 21 P. J. Flory, *Principles of Polymer Chemistry*, Cornell University Press, New York, 1953.
- 22 W. H. Stockmayer, *Journal of Chemical Physics*, 1944, **12**, 125–136.
- 23 L. C. Case, *Journal of Polymer Science*, 1960, **45**, 397–404.
- 24 H. M. J. a. E. Guth, *Journal of Chemical Physics*, 1943, **11**, 455–467.
- 25 N. C. Fitzkee and G. D. Rose, *Proceedings of the National Academy of Sciences of the United States of America*, 2004, **101**, 12497–12502.
- 26 R. P. Sijbesma, F. H. Beijer, L. Brunsveld, B. J. B. Folmer, J. Hirschberg, R. F. M. Lange, J. K. L. Lowe and E. W. Meijer, *Science*, 1997, **278**, 1601–1604.
- 27 D. C. Chow, W. K. Lee, S. Zauscher and A. Chilkoti, *Journal of the American Chemical Society*, 2005, **127**, 14122–14123.
- 28 T. Vermonden, J. van der Gucht, P. de Waard, A. T. M. Marcelis, N. A. M. Besseling, E. J. R. Sudholter, G. J. Fleer and M. A. C. Stuart, *Macromolecules*, 2003, **36**, 7035–7044.